Carbohydrate Polymers 74 (2008) 659–665

Contents lists available at ScienceDirect

Carbohydrate Polymers

journal homepage: www.elsevier.com/locate/carbpol

Biosynthesis of bacterial cellulose/multi-walled carbon nanotubes in agitated culture

Zhiyong Yan, Shiyan Chen, Huaping Wang *, Biao Wang, Jianming Jiang

State Key Laboratory for Modification of Chemical Fibers and Polymer Materials, Donghua University, 2999#, Rinmin North Road, Shanghai 201620, PR China

ARTICLE INFO

Article history:
Received 12 November 2007
Received in revised form 1 March 2008
Accepted 14 April 2008
Available online 27 April 2008

Keywords:
Bacterial cellulose
Multi-walled carbon nanotubes
Agitated culture

ABSTRACT

The morphology of bacterial cellulose (BC) is quite different in the static and agitated culture. In this study, the snow-like cellulose assemblies are synthesized in the agitated culture and the fibrous and rice-like cellulose assemblies are produced in the presence of multi-walled carbon nanotubes (MWNTs) in agitated culture. The microstructure of BC synthesized in agitated culture are investigated by scanning electron microscopy (SEM), Fourier transform infrared spectroscopy (FT-IR) and X-ray diffractometry (XRD). The analysis results reveal that the crystallinity index, crystallite size and cellulose I_α content for cellulose synthesized in agitated culture are lower than those for cellulose synthesized in static culture. The agitating stress influences the aggregation and crystallization of sub-elementary fibrils, further changes the intramolecular and intermolecular hydrogen bond patterns. The stress makes greater effect on BC synthesized in the absence of MWNTs than in the presence of MWNTs.

1. Introduction

Bacterial cellulose (BC) is produced by some kinds of acetic acid bacteria. BC demonstrates unique properties including high mechanical strength, high crystallinity, high water holding capacity and high porosity, which make it a very useful biomaterial in many different industrial processes such as in food and medical industries (Fontana et al., 1990; Iguchi, Yamanaka, & Budhiono, 2000; Klemm, Schumann, Udhardt, & Marsch, 2001).

There are two methods to produce BC, namely stationary and agitated culture. The macroscopic morphology of BC varies depending on the culture methods. The stationary culture results in the accumulation of a gelatinous membrane of cellulose at the air/liquid interface, while the agitated culture results in the fibrous suspensions, pellets, spheres or irregular masses (Chao, Ishida, Sugano, & Shoda, 2000; Czaja, Romanovicz, & Brown, 2004; Watanabe, Tabuchi, Morinaga, & Yoshinaga, 1998). The stationary culture conditions have been quite successfully investigated and described. However, it was reported that the agitated culture might be the most suitable technique for economical scale production (Ross, Mayer, & Benziman, 1991; Yoshinaga, Tonouchi, & Watanabe, 1997), although the agitated culture of *Acetobacter* strains causes many problems, among which strain instability, non-Newtonian behavior during mixing of BC, or proper oxygen supply are the most common (Hwang, Yang, Hwang, Pyun, & Kim, 1999; Jung, Park, & Chang, 2005; Kouda, Naritomi, Yano, & Yoshinaga, 1998; Kouda, Yano, & Yoshinaga, 1997; Kouda, Yano, Yoshinaga, Kaminoyama, & Kamiwano, 1996).

Moreover, the change of cultural conditions can influence the microstructure such as crystallinity, crystalline polymorphism, crystallite size, the cellulose I_α content and mechanical properties of BC. In static culture, the effects of the water-soluble agents and polysaccharides in culture media on the aggregation and crystallization of BC microfibrils were intensively studied (Ben-Hayyim & Ohad, 1965; Haigler, Brown, & Benziman, 1980; Seifert, Hesse, Kabrelian, & Klemm, 2004; Whitney, Brigham, & Darke, 1995; Yamamoto, Horii, & Hirai, 1996). The results revealed that the additives in static culture may delay the aggregation of cellulose microfibrils and prohibit the crystallization of cellulose microfibrils, decreasing the crystallite size, crystallinity index and cellulose I_α content. By adding silica sol into the static growth medium, the silica changed the elasticity and strength of BC (Yano, Maeda, Nakajima, Hagiwara, & Sawaguchi, 2008). However, few researches on the effects of additives in agitated culture were conducted.

Multi-walled carbon nanotubes (MWNTs) are nearly one-dimensional nanomaterials with a high aspect ratio, as well as superior mechanical and electrical properties (Avouris, 2002; Biercuk, Llaguno, Radosvljevic, Hyun, & Johnson, 2002; Iijima, 1991; Showkat et al., 2006). The MWNTs and BC fibrils, which are nanofibers, could be used as biomaterials such as artificial muscles, artificial blood vessels, respectively (Klemm et al., 2001; Vohrer, Kolaric, Haque, Roth, & Detlaff-Weglikowska, 2004). It can be expected that the BC/MWNTs composites will be used widely as biomaterials. It may be a good method to obtain the composites by in situ biosynthesis in the presence of MWNTs in culture medium. However, the MWNTs

* Corresponding author. Tel.: +86 21 67792958; fax: +86 21 67792726.
E-mail address: wanghp@dhu.edu.cn (H. Wang).

0144-8617/$ - see front matter Crown copyright © 2008 Published by Elsevier Ltd. All rights reserved.
doi:10.1016/j.carbpol.2008.04.028

in agitated medium can increase the viscosity of the broth, which may influence the morphology and microstructure of BC.

The effects of MWNTs on the structure of BC in static culture were studied (Yan et al., 2008). In this study, the acid-treated MWNTs were added to the agitated culture medium containing *Acetobacter xylinum* 1.1812 strain. We studied the morphology and microstructure of BC synthesized in agitated culture by light photographs, scanning electron microscopy (SEM), Fourier transform infrared spectroscopy (FT-IR) and X-ray diffractometry (XRD).

2. Experimental

2.1. Functionalization of MWNTs

The MWNTs (purity, >97%) were kindly provided by Tsinghua-Nafine Nano-Powder Commercialization Engineering Center, Beijing, China. Their outer diameters are 20–40 nm and their lengths are about 10–50 μm. MWNTs (400 mg) was suspended in 400 mL of a mixture of concentrated nitric acid (68%) and sulfuric acid (98%) (1:3 in volume ratio) and refluxed at 80 °C for 10 h. Then, the samples were filtered with PTFE (poly-tetrafluoroethylene) membrane with the pore size of 0.1 μm in deionized water and ultrasonicated in a 120 W and 59 kHz ultrasonic bath for 30 min prior to use.

2.2. BC culture media and condition

Acetobacter xylinum 1.1812 strain was kindly provided by Institute of Microbiology, Chinese Academy of Science. Two types of culture media were used: the Hestrin–Schramm culture medium (HS) (2.5 w/v% D-glucose, 0.5 w/v% peptone, 0.5 w/v% yeast extract, 0.115 w/v% citric acid, and 0.25 w/v% disodium hydrogen phosphate) and MWNT–HS medium (in the presence of final 0.005 w/v% MWNTs in HS medium). These culture media were sterilized at 121 °C in autoclave for 30 min by autoclaving and poured into Erlenmeyer flasks. These cultures were incubated in static or on a rotary shaker operating at rotational speed of 150 rpm, for 10 days at 28 °C. The synthesized cellulose was separated from the medium by filtration and boiled in 1% sodium hydroxide solution for 30 min in order to remove cells and medium embedded in the cellulose material, then rinsed 3 days to pH 7 in deionized water.

2.3. Light photographs and SEM observation

The never-dried samples in water were taken photos. The samples were freeze-dried and coated with gold palladium by cathodic spreading in a Polaron E 5100 coater and examined with a JSM-5600LV (JEOL, Japan) scanning electron microscope.

2.4. X-ray diffractometry

The air-dried thin-membranes were placed on an aluminum plate. X-ray diffraction was recorded with a Rigaku-D/Max-2550 PC diffractometer. The radiation was Ni-filtered Cu K_α of wavelength 1.54056 Å. The operating voltage and current were 40 kV and 30 mA, respectively. Angular scanning was continued 5°–60° at 1°/min and data were collected using 2-step scan mode with angular intervals of 0.02°. The diffraction profile was processed by computer-aided fitting analysis. The interplanar distances of crystallographic planes (d-spacings) were calculated by Bragg law. The crystal sizes of the cellulose samples were calculated in the direction perpendicular to the $(1\bar{1}0)$, (110) and (200) crystallographic planes from the line-broadening data by Scherrer equation:

$$D_{(hkl)} = \frac{K\lambda}{\beta_0 \cos\theta} \quad (1)$$

where β_0 is the full width half maximum, in radian, of the reflections corrected for instrumental broadening and λ is the wavelength of the employed X-ray radiation, 1.54056 Å. The crystallite index (CrI^{XRD}) was empirical method for native cellulose:

$$CrI^{XRD} = \frac{I_{200} - I_{am}}{I_{200}} \times 100 \quad (2)$$

where I_{200} is the maximum intensity of the (200) lattice diffraction and I_{am} is the intensity diffraction at $2\theta = 18°$ (Focher et al., 2001).

2.5. FT-IR spectroscopy

The acid-treated MWNTs were well mixed with potassium bromide (KBr) powder, dried at 50 °C under vacuum, and pressed into a small tablet. The bacterial cellulose thin-membrane with or without MWNTs dried at 40 °C under vacuum. FT-IR spectra were recorded on a Nicolet model 6000 C equipped with a MCT detector in the absorption mode with a resolution of 4 cm^{-1} in the range of 4000–400 cm^{-1}. The mass fraction of cellulose $I_\alpha f_\alpha^{IR}$, was estimated from the Eq. (3) (Imai & Sugiyama, 1998),

$$f_\alpha^{IR} = \frac{A_{750}}{A_{750} + kA_{710}} \quad (3)$$

Where A_x is the integrated absorption at the corresponding wavenumber and k is the constant ($k = 0.16$).

3. Results and discussion

3.1. The morphology of BC

The macroscopic morphology of BC varies depending on the culture methods (Hestrin & Schramm, 1954; Watanabe et al., 1998). Most of the *A.* xylinum strains used worldwide in research cellulose synthesize statically in the form of a gelatinous membrane at the liquid/air interface (Borzani & Desouza, 1995; Klemm et al., 2001). Fig. 1a shows the never-dried gelatinous BC membrane produced in static culture (S-BC). It is white and semitransparent after purification. It was reported that many particles of various size (10 μm–1 mm) and various shapes (spherical, ellipsoidal, stellate or fibrous) were accumulated in well-dispersed suspension in the agitated culture (Hestrin & Schramm, 1954; Yoshinaga et al., 1997). However, in this study, the BC assemblies produced in agitated culture (Ag-BC) are snow-like, which are shown in Fig. 1b. There is a long thread connecting the small flocky fibrils in every BC assembly. The additives such as polysaccharides and hemicelluloses could interact with the BC microfibrils and change the morphology in static culture (Tokoh, Takabe, Fujita, & Saiki, 1998; Uhlin, Atalla, & Thompson, 1995; Whitney, Brigham, Darke, Reid, & Gidley, 1998). In the presence of acid-treated MWNTs, the BC assemblies synthesized in agitated culture (Ag-MWNT–BC) are fibrous and rice-like as shown in Fig. 1c. The shapes are not uniformly regular. The fibrous assemblies are 1–2 mm wide and 3–15 mm long, and the rice-like assemblies are 2–3 mm wide and 2–5 mm long. In the both assemblies, the BC and MWNTs form the skin-core structure. The MWNTs are packed as the core of the assemblies. It seems that the rice-like assemblies look blacker than the fibrous assemblies because there are more MWNTs in the core of rice-like assemblies.

In static culture, increasing in the thickness of cellulose membrane is due to the formation of new cellulose layers at the membrane/air interface because there is enough oxygen in air needed by the aerobic *A.* xylinum (Borzani & Desouza, 1995). In contrast, in agitated culture, cellulose is synthesized in deep media and the

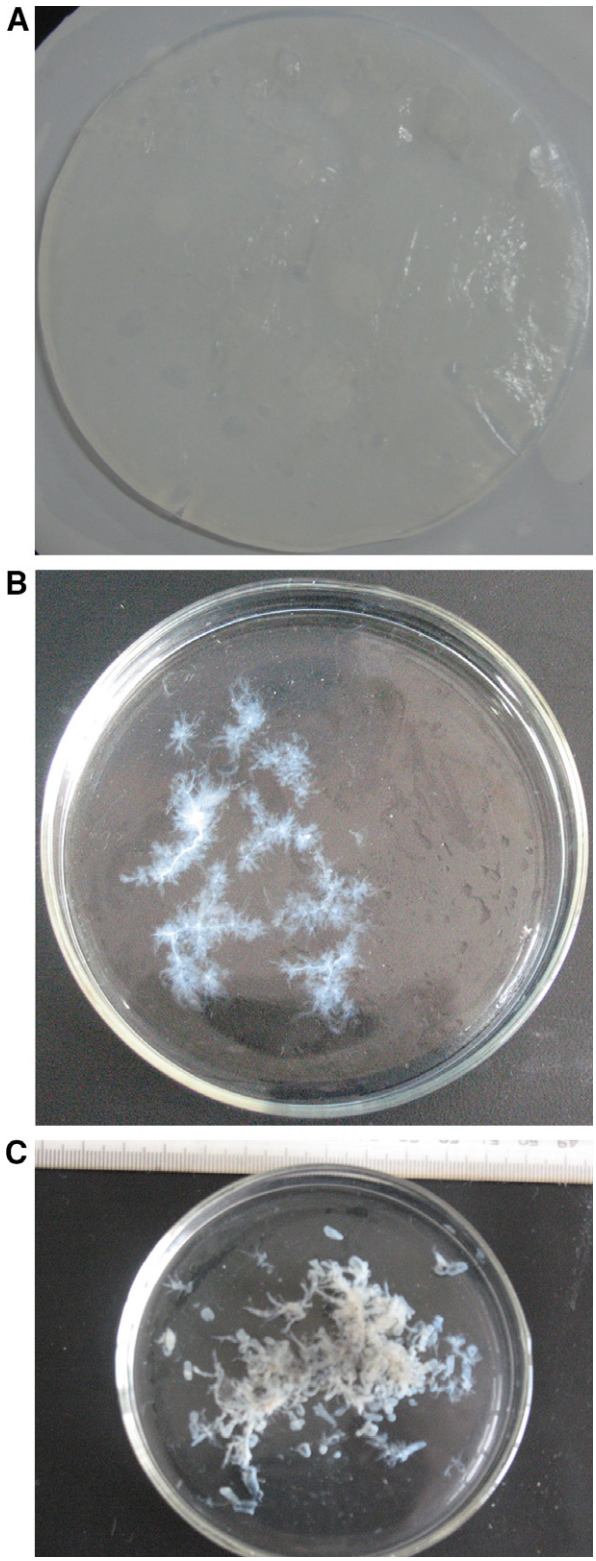

Fig. 1. The photographs of never-dried (a) S-BC; (b) Ag-BC and (c) Ag-MWNT–BC.

production rate and yield of BC are proportional to the oxygen transfer rate and oxygen transfer coefficient (Kouda, Naritomi, Yano, & Yoshinaga, 1997). The cells attached to the surface of bubbles existing in the agitated broth start to reproduce and synthesize sub-elementary cellulose fibrils (Czaja et al., 2004). The strong stress forces in agitated culture change the aggregation of sub-elementary fibrils and form the irregular shape assemblies. The MWNTs with a high aspect ratio in the agitated medium entangle with each other and form agglomerates. Then, the cells gather around the MWNTs agglomerates and assemble the fresh BC along the agglomerates. The MWNTs are packed in the core and the shapes of BC assemblies depend largely on the shape of MWNTs agglomerates, forming the irregular rice-like and fibrous assemblies.

In order to observe the BC microfibrils, we obtain their SEM micrographs. Fig. 2a shows the SEM image of S-BC. It reveals the reticulated structure consisting of ultrafine fibrils with 60–100 nm width. However, the Ag-BC appears also reticulated structure consisting of band-like assemblies with 0.6–1.2 μm width as shown in Fig. 2b. The Ag-BC bands twist and curl apparently, in contrast, the S-BC microfibrils are straighter. The twist of bands may be caused by the agitating force of the turbulent flow in agitated broth. Fig. 2c shows the SEM image of Ag-MWNT–BC. The width of fibrils change from 1–2 mm in never-dried state to 1–1.5 μm in air-dried state. The fibrous assemblies are composed of 10 of cellulose microfibrils which twist up and pack the MWNTs as the core. Fig. 2d shows the cross-section SEM image of Ag-MWNT–BC. It reveals that the MWNTs in the core are denser than those in the fringe. The gradual dispersion of MWNTs along the radial direction indicates that the BC assembles layer-by-layer with culture time increasing.

3.2. XRD analysis

In order to compare the microstructural changes in cellulose samples from the different culture conditions and especially to estimate if the shaking force causes any disturbance in the crystallization process, X-ray diffraction was used. Fig. 3 shows the X-ray diffraction patterns of acid-treated MWNTs, S-BC, Ag-BC and Ag-MWNT–BC. The diffraction pattern for acid-treated MWNTs exhibits two main peaks at 25.82° and 42.72°, corresponding to the (002) and (100) reflection, respectively (Wang et al., 2005). The S-BC crystallites show main peaks at about 14.22° and 22.53°, corresponding to the crystallographic plane of $(1\bar{1}0)$ and (200), respectively (Tokoh et al., 1998). The Ag-BC crystallites reveal the main peaks at 14.87° and 23.00°, corresponding to the $(1\bar{1}0)$ and (200) plane, respectively. It indicates that the S-BC and Ag-BC samples are the typical crystalline forms of cellulose I (Oh, Yoo, Shin, & Kim, 2005; Uhlin et al., 1995). The Ag-MWNT–BC crystallites show the main peaks for cellulose I at 14.88°, 17.22° and 23.01°, and the weak peak for MWNTs at 25.89°, which indicates that a large number of MWNTs are embedded into the BC as shown in Fig. 1c. The d-spacings calculated with Bragg law are listed in Table 1.

According to Atalla & VanderHart (1984), native celluloses generally consist of two crystalline phases, namely triclinic cellulose I_α and monoclinic I_β (Sugiyama, Vuong, & Chanzy, 1991b). The ratio I_α to I_β depends on the cellulose source (Akerholm, Hinterstoisser, & Salmen, 2004; Ciolacu, 2007; Imai, Sugiyama, Itoh, & Horii, 1999; Udhardt, Hesse, & Klemm, 2005). The d-spacing data are reported to reflect the cellulose I_α and I_β fractional ratio, since each peak contains a combination from the I_α and I_β diffractions whose d-spacings are slightly different (Wada and Okano,2001; Wada, Okano, & Sugiyama, 1997). The d-spacing for $(1\bar{1}0)$ plane is a combination of (100) plane of I_α with a 6.13 Å spacing and the $(1\bar{1}0)$ plane of I_β with a 6.03 Å spacing (Wada et al., 1997). The smaller value of d-spacing for $(1\bar{1}0)$ plane means the lower cellulose I_α content in cellulose. The d-spacing for $(1\bar{1}0)$ plane in S-BC, Ag-MWNT–BC and Ag-BC is 6.22, 6.16 and 5.95 Å, respectively. It suggests the cellulose I_α content in Ag-BC is the lowest. The crystallite sizes calculated from the $(1\bar{1}0)$, (110) and (200) plane using Eq. (1) are listed in Table 1. They clearly demonstrate the existence of smallest crystallite size in Ag-BC. The results of CrI^{XRD} calculated by Eq. (2) are listed in Table 1. The data reveal that the CrI^{XRD} for Ag-BC is the lowest.

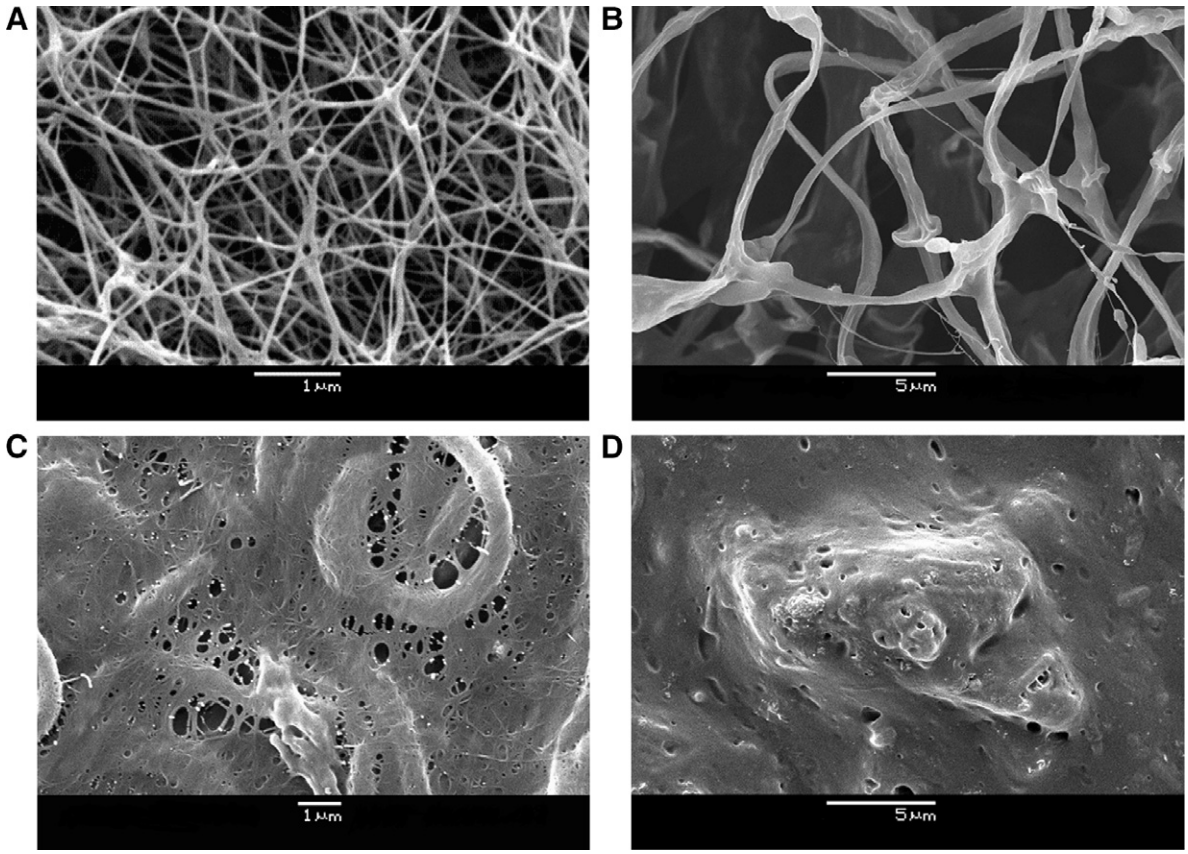

Fig. 2. SEM images of (a) freeze-dried S-BC, (b) freeze-dried Ag-BC, (c) air-dried Ag-MWNT–BC and (d) the cross-section of freeze-dried fibrous Ag-MWNT–BC.

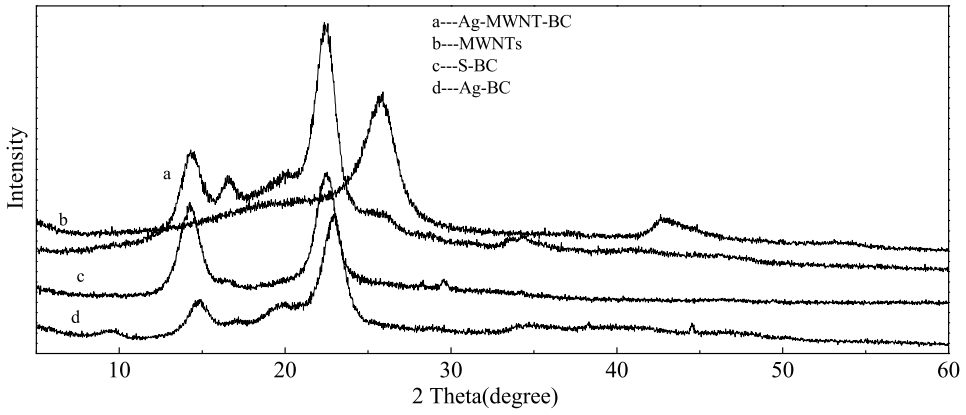

Fig. 3. X-ray diffraction patterns obtained from MWNTs, S-BC, Ag-BC and Ag-MWNT–BC.

Table 1
d-Spacings, crystallite sizes and crystallinity index of S-BC, Ag-BC and Ag-MWNT–BC determined from X-ray diffractograms

Samples	d-Spacings (Å)			Crystallite sizes (Å)			CrI^{XRD} (%)
	$1\bar{1}0$	110	200	$1\bar{1}0$	110	200	
S-BC	6.22	5.28	3.94	62.61	86.17	62.29	81.65
Ag-BC	5.95	5.19	3.86	62.99	45.58	51.06	67.17
Ag-MWNT–BC	6.16	5.35	3.97	53.87	50.75	54.32	76.21

The conditions of stress occurring during agitation appear to strongly interfere with the process of nascent microfibrils crystallization, decreasing the crystallinity and crystallite size, favouring the formation of cellulose I_β, the more stable allomorph (Czaja et al., 2004; Watanabe et al., 1998). The smaller crystallite size and lower CrI^{XRD} for Ag-BC comparing to Ag-MWNT–BC means that the effect of agitating stress in the absence of MWNTs is more intensive than in the presence of MWNTs in agitated culture. This can be explained that the sub-elementary fibrils may attach to the MWNTs and be more stable in the strong agitating stress.

3.3. FT-IR analysis

Fig. 4a shows the FT-IR spectra in the O–H-stretching vibration regions of the samples. The band at 3419 cm^{-1} for MWNTs is attributed to the presence of hydroxyl groups (–OH). It indicates the oxidation of MWNTs by concentrated H_2SO_4/HNO_3. Since bac-

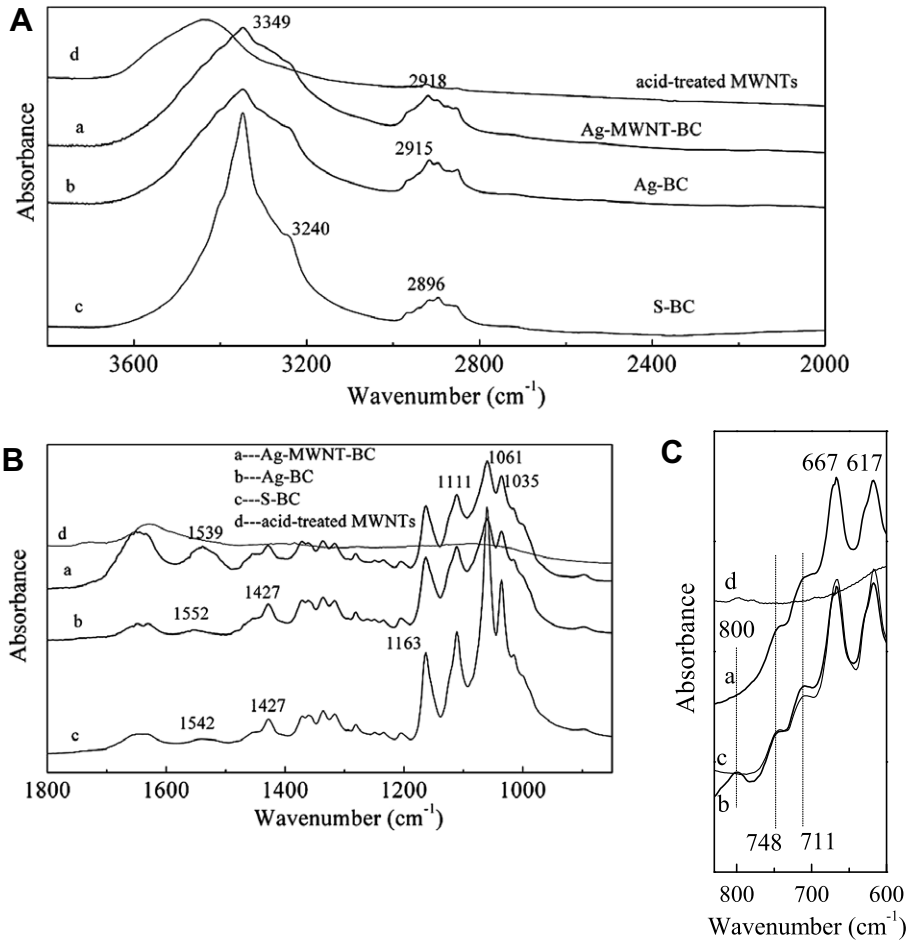

Fig. 4. FT-IR spectrograms obtained from acid-treated MWNTs, S-BC, Ag-BC and Ag-MWNT–BC in the range of (a) 3800–2000, (b) 1800–850 and (c) 810–600 cm^{-1}.

terial cellulose contains a large number of highly polar hydroxyl groups, the molecular chains interact by intramolecular and intermolecular hydrogen bonds (Hofstetter, Hinterstoisser, & Salmen, 2006; Kataoka & Kondo, 1998; Marechal & Chanzy, 2000; Watanabe, Morita, & Ozaki, 2007). The dominating signal for BC is at 3349 cm^{-1}, which is attributed to the intramolecular hydrogen bond for 3O...H–O5 (Oh et al., 2005). It is the sharpest and most intensive absorbance peak in S-BC, while it becomes the broader in both Ag-BC and Ag-MWNT–BC, which implies that there are more hydrogen-bonding patterns in Ag-BC and Ag-MWNT–BC. In S-BC, there is a significant peak at 3240 cm^{-1}, which is attributed to the intermolecular hydrogen bond, corresponding to the contributions from cellulose I_α (Sugiyama, Persson, & Chanzy, 1991a). In contrast, there is only a relative weak absorbance peak near 3240 cm^{-1} in Ag-BC and Ag-MWNT–BC. The phenomena demonstrate that there is more cellulose I_α content in S-BC comparing to that in the Ag-BC and Ag-MWNT–BC. It implies that the agitating stress interferes with the formation of intramolecular and intermolecular hydrogen bonds in sub-elementary cellulose fibrils and disturbs their aggregation and crystallization. Fig. 4b shows the FT-IR spectra in the C–O-stretching vibration regions. The band at 1163 cm^{-1} is attributed to the C1–O–C4 glycosidic link, and the bands at 1111, 1061 and 1035 cm^{-1} are assigned to the vibrations of C2–O2, C3–O3 and C6–O6, respectively (Kacurakova, Smith, Gidley, & Wilson, 2002; Marechal & Chanzy, 2000). Their modes are similar, however, the intensity at 1061 cm^{-1} in S-BC is much higher relative to that in the Ag-BC and Ag-MWNT–BC. It suggests that there are stronger intramolecular hydrogen bonds for 3O...H–O5 in BC, which is consistent with the FT-IR spectrum in the O–H-stretching vibration region. While no obvious difference between Ag-BC and Ag-MWNT–BC is observed in the C–O-stretching vibration regions.

The crystallinity index (CrI^{IR}) of cellulose could also be evaluated by the intensity ratio H_{1428}/H_{896} between FT-IR absorptions at 1428 and 896 cm^{-1} (Akerholm et al., 2004). The absorbance at 1428 and 896 cm^{-1}, which are assigned to CH_2 bending mode and deformation of anomeric CH, respectively (Kataoka & Kondo, 1998), are sensitive to the amount of crystalline versus amorphous structure in cellulose. The values of CrI^{IR} for the samples are listed in Table 2. It shows that the CrI^{IR} of S-BC is much higher than that of Ag-BC and Ag-MWNT–BC. The results are consistent with the CrI^{XRD}. It implies that the agitating stress influences with the aggregation and crystallization of cellulose sub-elementary microfibrils. The data also indicate that the effect of the agitating stress in the absence of MWNTs is more obvious than in the presence of MWNTs in agitated culture.

The absorption band at 748 cm^{-1} is attributed to the contribution of cellulose I_α, whereas 711 cm^{-1} corresponds to the contribution from cellulose I_β shown in Fig. 4c (Debzi, Chanzy, Sugiyama,

Table 2
The values of f_α^{IR} and CrI^{IR}

Sample	f_α^{IR}	CrI^{IR}
S-BC	55.62%	5.13
Ag-BC	37.46%	2.23
Ag-MWNT–BC	41.73%	2.56

Tekely, & Excoffier, 1991; Debzi, Marchessault, Excoffier, & Chanzy, 1999; Sugiyama et al., 1991a). To determinate the cellulose I_α content quantitatively, the absorption bands at 748 and 711 cm^{-1} were deconvoluted by using Lorenzian curving fitting analysis on the original spectra. The mass fraction of cellulose I_α could be calculated according to the Eq. (3). The values of f_α^{IR} are listed in Table 2. The data indicate that the cellulose I_α content in S-BC is higher than that in Ag-BC and Ag-MWNT–BC. It agrees with the values of d-spacings from X-ray diffractograms.

4. Conclusion

In conclusion, *A.* xylinum 1.1812 strain has been found to effectively synthesize cellulose in agitated culture. Many other strains of *Acetobacter* undergo mutation to non-cellulose producing cells under agitation (Czaja et al., 2004), however, with the *A.* xylinum 1.1812 strain, mutations to the non-cellulose state do not occur. The snow-like cellulose assemblies are produced in agitated culture and the fibrous and rice-like cellulose assemblies are synthesized in the presence of MWNTs in agitated culture. The nascent sub-elementary fibrils attached MWNTs and packed them as the core of the cellulose assemblies. The Ag-BC and Ag-MWNT–BC microfibrils twist and curl apparently, wider than S-BC microfibrils. The crystallite size for Ag-BC and Ag-MWNT–BC are smaller than that for S-BC. The crystallinity index and cellulose I_α content for Ag-BC and Ag-MWNT–BC are also lower than that for S-BC. It may be attributed to the agitating stress which could interfere with the aggregation and crystallization of BC microfibrils, change the intramolecular and intermolecular hydrogen-bonding patterns. The effect of the agitating stress on BC synthesized in the absence of MWNTs is more intensive than on BC synthesized in the presence of MWNTs, which may be that the sub-elementary fibrils attaching the MWNTs are more stable in agitated culture.

Acknowledgements

This work was financially supported by the 111 project (B07024), School Fund and New Century Excellent Talents in University (NCET-05-0420).

References

Akerholm, M., Hinterstoisser, B., & Salmen, L. (2004). Characterization of the crystalline structure of cellulose using static and dynamic FT-IR spectroscopy. *Carbohydrate Research, 339*(3), 569–578.

Atalla, R. H., & VanderHart, D. L. (1984). Native cellulose: A composite of two distinct crystalline forms. *Science, 223*, 283–285.

Avouris, P. (2002). Carbon nanotube electronics. *Chemical Physics, 281*(2-3), 429–445.

Ben-Hayyim, G., & Ohad, I. (1965). Synthesis of cellulose by *Acetobacter xylinum*. *The Journal of Cell Biology, 25*, 191–207.

Biercuk, M. J., Llaguno, M. C., Radosvljevic, M., Hyun, J. K., & Johnson, A. T. (2002). Carbon nanotube composites for thermal management. *Applied Physics Letters, 80*, 15.

Borzani, W., & Desouza, S. J. (1995). Mechanism of the film thickness increasing during the bacterial production of cellulose on non-agitated liquid-media. *Biotechnology Letters, 17*(11), 1271–1272.

Chao, Y. P., Ishida, T., Sugano, Y., & Shoda, M. (2000). Bacterial cellulose production by *Acetobacter xylinum* in a 50-L internal-loop airlift reactor. *Biotechnology and Bioengineering, 68*(3), 345–352.

Ciolacu, D. (2007). On the supramolecular structure of cellulose allomorphs after enzymatic degradation. *Journal of Optoelectronics and Advanced Materials, 9*(4), 1033–1037.

Czaja, W., Romanovicz, D., & Brown, R. M. (2004). Structural investigations of microbial cellulose produced in stationary and agitated culture. *Cellulose, 11*(3-4), 403–411.

Debzi, E. M., Chanzy, H., Sugiyama, J., Tekely, P., & Excoffier, G. (1991). The $I_\alpha \rightarrow I_\beta$ transformation of highly crystalline cellulose by annealing in various mediums. *Macromolecules, 24*(26), 6816–6822.

Debzi, E. M., Marchessault, R. H., Excoffier, G., & Chanzy, H. (1999). Flash hydrolysis deinking of laser print using degradable toner resin. *Macromolecular Symposia, 143*, 243–255.

Focher, B., Palma, M. T., Canetti, M., Torri, G., Cosentino, C., & Gastaldi, G. (2001). Structural differences between non-wood plant celluloses: Evidence from solid state NMR, vibrational spectroscopy and X-ray diffractometry. *Industrial Crops and Products, 13*, 193–208.

Fontana, J. D., de Souza, A. M., Fontana, C. K., Torriani, I. L., Moreschi, J. C., Gallotti, B. J., et al. (1990). Acetobacter cellulose pellicle as a temporary skin substitute. *Applied Biochemistry Biotechnology*, 253–264.

Haigler, C. H., Brown, R. M., Jr., & Benziman, M. (1980). Calcofluor white ST alters the in vivo assembly of cellulose microfibrils. *Science, 210*(21), 903–906.

Hestrin, S., & Schramm, M. (1954). Synthesis of cellulose by *Acetobacter xylinum*. II. Preparation of freeze-dried cells capable of polymerizing glucose to cellulose. *Journal of Biochemistry, 58*, 345–352.

Hofstetter, K., Hinterstoisser, B., & Salmen, L. (2006). Moisture uptake in native cellulose-the roles of different hydrogen bonds: A dynamic FT-IR study using deuterium exchange. *Cellulose, 13*(2), 131–145.

Hwang, J. W., Yang, Y. K., Hwang, J. K., Pyun, Y. R., & Kim, Y. S. (1999). Effects of pH and dissolved oxygen on cellulose production by *Acetobacter xylinum* BRC5 in agitated culture. *Journal of Bioscience and Bioengineering, 88*(2), 183–188.

Iguchi, M., Yamanaka, S., & Budhiono, A. (2000). Bacterial cellulose – A masterpiece of nature's arts. *Journal of Materials Science, 35*(2), 261–270.

Iijima, S. (1991). Helical microtubules of graphitic carbon. *Nature, 354*, 56–58.

Imai, T., & Sugiyama, J. (1998). Nanodomains of I alpha and beta cellulose in algal microfibrils. *Macromolecules, 31*(18), 6275–6279.

Imai, T., Sugiyama, J., Itoh, T., & Horii, F. (1999). Almost pure I-alpha cellulose in the cell wall of Glaucocystis. *Journal of Structural Biology, 127*(3), 248–257.

Jung, J. Y., Park, J. K., & Chang, H. N. (2005). Bacterial cellulose production by Gluconacetobacter hansenii in an agitated culture without living non-cellulose producing cells. *Enzyme and Microbial Technology, 37*(3), 347–354.

Kacurakova, M., Smith, A. C., Gidley, M. J., & Wilson, R. H. (2002). Molecular interactions in bacterial cellulose composites studied by 1D FT-IR and dynamic 2D FT-IR spectroscopy. *Carbohydrate Research, 337*(12), 1145–1153.

Kataoka, Y., & Kondo, T. (1998). FT-IR microscopic analysis of changing cellulose crystalline structure during wood cell wall formation. *Macromolecules, 31*(3), 760–764.

Klemm, D., Schumann, D., Udhardt, U., & Marsch, S. (2001). Bacterial synthesized cellulose – artificial blood vessels for microsurgery. *Progress in Polymer Science, 26*(9), 1561–1603.

Kouda, T., Naritomi, T., Yano, H., & Yoshinaga, F. (1997). Effects of oxygen and carbon dioxide pressures on bacterial cellulose production by Acetobacter in aerated and agitated culture. *Journal of Fermentation and Bioengineering, 84*(2), 124–127.

Kouda, T., Naritomi, T., Yano, H., & Yoshinaga, F. (1998). Inhibitory effect of carbon dioxide on bacterial cellulose production by *Acetobacter* in agitated culture. *Journal of Fermentation and Bioengineering, 85*(3), 318–321.

Kouda, T., Yano, H., & Yoshinaga, F. (1997). Effect of agitator configuration on bacterial cellulose productivity in aerated and agitated culture. *Journal of Fermentation and Bioengineering, 83*(4), 371–376.

Kouda, T., Yano, H., Yoshinaga, F., Kaminoyama, M., & Kamiwano, M. (1996). Characterization of non-Newtonian behavior during mixing of bacterial cellulose in a bioreactor. *Journal of Fermentation and Bioengineering, 82*(4), 382–386.

Marechal, Y., & Chanzy, H. (2000). The hydrogen bond network in I beta cellulose as observed by infrared spectrometry. *Journal of Molecular Structure, 523*, 183–196.

Oh, S. Y., Yoo, D. I., Shin, Y., & Kim, H. C. (2005). Crystalline structure analysis of cellulose treated with sodium hydroxide and carbon dioxide by means of X-ray diffraction and FTIR spectroscopy. *Carbohydrate Research, 340*, 2376–2391.

Ross, P., Mayer, R., & Benziman, M. (1991). Cellulose biosynthesis and function in bacteria. *Microbiological Reviews, 55*(1), 35–38.

Seifert, M., Hesse, S., Kabrelian, V., & Klemm, D. (2004). Controlling the water content of never dried and reswollen bacterial cellulose by the addition of water-soluble polymers to the culture medium. *Journal of Polymer Science Part A – Polymer Chemistry, 42*(3), 463–470.

Showkat, A. M., Lee, K. P., Gopalan, A. I., Kim, S. H., Choi, S. H., & Sohn, S. H. (2006). Characterization and preparation of new multiwall carbon nanotube/conducting polymer composites by in situ polymerization. *Journal of Applied Polymer Science, 101*(6), 3721–3729.

Sugiyama, J., Persson, J., & Chanzy, H. (1991a). Combined infrared and electron diffraction study of the polymorphism of native celluloses. *Macromolecules, 24*(9), 2461–2466.

Sugiyama, J., Vuong, R., & Chanzy, H. (1991b). Electron diffraction study on the two crystalline phases occurring in native cellulose from an algal cell wall. *Macromolecules, 24*(14), 4168–4175.

Tokoh, C., Takabe, K., Fujita, M., & Saiki, H. (1998). Cellulose synthesized by *Acetobacter xylinum* in the presence of acetyl glucomannan. *Cellulose, 5*(4), 249–261.

Udhardt, U., Hesse, S., & Klemm, D. (2005). Analytical investigations of bacterial cellulose. *Macromolecular Symposia, 223*, 201–212.

Uhlin, K. I., Atalla, R. H., & Thompson, N. S. (1995). Influence of hemicelluloses on the aggregation patterns of bacterial cellulose. *Cellulose, 2*(2), 129–144.

Vohrer, U., Kolaric, I., Haque, M. H., Roth, S., & Detlaff-Weglikowska, U. (2004). Carbon nanotube sheets for the use as artificial muscles. *Carbon, 42*(5-6), 1159–1164.

Wada, M., & Okano, T. (2001). Localization of I-alpha and I-beta phases in algal cellulose revealed by acid treatments. *Cellulose, 8*(3), 183–188.

Wada, M., Okano, T., & Sugiyama, J. (1997). Synchrotron-radiated X-ray and neutron diffraction study of native cellulose. *Cellulose, 4*(3), 221–232.

Wang, Z., Ba, D. C., Liu, F., Cao, P. J., Yang, T. Z., Gu, Y. S., et al. (2005). Synthesis and characterization of large area well-aligned carbon nanotubes by ECR-CVD without substrate bias. *Vacuum, 77*(2), 139–144.

Watanabe, A., Morita, S., & Ozaki, Y. (2007). Temperature-dependent changes in hydrogen bonds in cellulose I alpha studied by infrared spectroscopy in combination with perturbation-correlation moving-window two-dimensional correlation spectroscopy: Comparison with cellulose I beta. *Biomacromolecules, 8*(9), 2969–2975.

Watanabe, K., Tabuchi, M., Morinaga, Y., & Yoshinaga, F. (1998). Structural features and properties of bacterial cellulose produced in agitated culture. *Cellulose, 5*(3), 187–200.

Whitney, S. E. C., Brigham, J. E., & Darke, A. H. (1995). In vivo assembly of cellulose/xyloglucan networks: Ultrastructural and molecular aspects. *Plant Journal, 8*, 491–504.

Whitney, S. E. C., Brigham, J. E., Darke, A. H., Reid, J. S. G., & Gidley, M. J. (1998). Structural aspects of the interaction of mannan-based polysaccharides with bacterial cellulose. *Carbohydrate Research, 307*(3-4), 299–309.

Yamamoto, H., Horii, F., & Hirai, A. (1996). In situ crystallization of bacterial cellulose. 2. Influences of different polymeric additives on the formation of celluloses I-alpha and I-beta at the early stage of incubation. *Cellulose, 3*(4), 229–242.

Yan, Z., Chen, S., Wang, H., Wang, B., Wang, C., & Jiang, J. (2008). Cellulose synthesized by *Acetobacter xylinum* in the presence of multi-walled carbon nanotubes. *Carbohydrate Research, 343*(1), 73–80.

Yano, S., Maeda, H., Nakajima, M., Hagiwara, T., & Sawaguchi, T. (2008). Preparation and mechanical properties of bacterial cellulose nanocomposites loaded with silica nanoparticles. *Cellulose, 15*(1), 111–120.

Yoshinaga, F., Tonouchi, N., & Watanabe, K. (1997). Research progress in production of bacterial cellulose by aeration and agitation culture and its application as a new industrial material. *Bioscience Biotechnology and Biochemistry, 61*(2), 219–224.